JOURNAL OF MATERIALS SCIENCE 6 (1971) 439–447

Structures of Some 17% Cr(Mn, N) Stainless Steels

P. L. AHUJA, B. N. HALDER, S. S. BHATNAGAR
National Metallurgical Laboratory, Jamshedpur-7, India

A study of the structures of 17 wt.% Cr(Mn, N) stainless steels has been made with the help of X-ray diffraction, optical and electron microscopic techniques. It reveals that these steels become entirely austenitic when 10% manganese or more is present in a steel that contains about 0.4% nitrogen and 0.1% carbon. No precipitation other than the grain boundary carbides is observed on prolonged exposure to high temperatures.

Below 10% manganese, an unstable austenite is formed which undergoes a series of transformations at different temperatures. The mode of these transformations has been studied in detail from 1400 to 700°C. A possible mechanism of transformation is discussed.

1. Introduction

Nickel-free stainless steels are of interest to countries which do not possess large deposits of nickel. Since India does not possess any proven deposit of nickel, development of nickel-free stainless steels was undertaken at the National Metallurgical Laboratory. During the course of this work, some interesting transformations were encountered in the duplex range of the 17% Cr(Mn, N) steels when subjected to isothermal treatment at different temperatures [1].

The conventional steels containing 17 wt. % Cr consist, at room temperature and in the equilibrium state, of body-centred cubic phase (α-ferrite) and carbides, but on progressive heating, they undergo a partial transformation to face-centred cubic γ-phase (austenite) up to a maximum of 1100°C, above which it regresses and, at about 1300°C, a single homogeneous body-centred cubic phase (δ-ferrite) is again obtained and remains stable up to the solidus. These high-temperature transformations are the cause of the double loop separating the gamma and the alpha (or delta) regions in the Fe-Cr equilibrium diagram [2].

Increasing amounts of carbon and nitrogen contribute strongly to austenite formation. The gamma-promoting influence of carbon and nitrogen is practically equivalent. Chromium strongly promotes, and manganese weakly promotes, delta ferrite formation in the range of 1150 to 1300°C. One half per cent chromium in excess of the limit of austenite stability at 1260°C will produce approximately 3% of the delta ferrite. Increasing the nitrogen content by approximately 0.05% is as effective as an increase of 1% nickel in enhancing austenite formation at 1300°C. Either addition permits an increase in chromium content of approximately 0.6% without decrease in austenite stability. Increasing amounts of both chromium and manganese are effective in enhancing the solid solubility of these steels for nitrogen [3].

From a commercial point of view, the precipitation of delta ferrite is known to seriously affect the hot-working characteristics of these steels. The presence of delta ferrite also impairs the deep-drawing properties of the austenitic steels. Its presence, however, is essential to produce a controlled-transformation stainless steel that can be heat-treated to give high strength [4].

In view of the fact that these structural modifications resulting from the addition of manganese and nitrogen in varying amounts to the conventional 17% Cr steels have a pronounced influence on their properties, the establishment of the relationship between the manganese and nitrogen contents and the structural modification is essential in order to obtain a comprehensive understanding of the characteristics of these steels.

2. Experimental Procedure

Heats of $\approx$ 10 kg ingot capacity were made in an air-melting basic-lined high-frequency induction

furnace, using Lowmoor iron, low-carbon ferro-chrome, nitrided ferro-chrome and nitrided electrolytic manganese. The electrolytic manganese was dehydrogenated by keeping it at 500°C for 2 h before nitriding. Loss of nitrogen during pouring was prevented by using the capping technique devised at the National Metallurgical Laboratory [1]. The ingots were hot-forged at 1250°C and rolled to sheets of 1.57 mm thickness.

All the samples were given a standard anneal in vacuum which consisted of heating at 1100°C for 30 min, followed by water-quenching. They were then heated in vacuum for different periods of time at temperatures ranging from 1400 to 700°C, after which they were again water-quenched. The corresponding structures were examined by microscopic and X-ray analysis.

A number of specimens was transformed directly from the standard annealing temperature of 1100°C to the various heat-treatment temperatures and the results obtained were found to be similar to those which had been subjected to an intermediate water-quench.

To reveal the microstructure, the polished samples were etched in various mixtures of picric and hydrochloric acids dissolved in alcohol, the proportions being varied according to the requirement for a particular specimen. Carbon extraction replicas were prepared from polished and etched surfaces for transmission electron-microscopic study of the samples. Hardness determination of the phases was made with a GKN Microhardness Tester using a load of 30 g.

For X-ray examination, thin strips were cut from the heat-treated sheets, smoothed and electropolished in a perchloric acid (20%)–butyl-cellosolve (10%)–alcohol electrolyte, using an annular stainless steel cathode at a current density of 0.04 amp/cm². The thin cylindrical wires thus obtained were suitable for direct mounting in a powder camera.

Precipitates were extracted electrolytically from the transformed samples by an electrolyte containing 60 g ammonium chloride and 160 g citric acid per litre of distilled water. The potential drop across the electrodes was maintained at 1.0 V and current density at 0.04 amp/cm². The precipitate was recovered from the electrolyte by centrifuging the solution and analysed by X-ray powder technique.

TABLE I Chemical composition of steels (wt.%, bal. Fe)

Steel	Cr	Mn	C	N	Si	S	P
S3	16.9	6.5	0.037	0.34	0.13	0.012	0.015
S4	17.1	8.3	0.049	0.39	0.12	0.010	0.009
S5	17.0	10.3	0.054	0.38	0.12	0.012	0.012
S6	17.2	12.7	0.063	0.37	0.15	0.011	0.010
S7	16.8	15.7	0.072	0.31	0.15	0.009	0.008
S8	17.1	16.9	0.108	0.41	0.15	0.014	0.011

3. Results

Table I shows the chemical analysis report of the six steels used for this investigation.

X-ray analysis of the samples annealed at 1100°C for 30 min showed that the steels S3 and S4 were duplex in structure, whereas steels with 10.3% Mn and above became entirely austenitic. This was confirmed by varying the holding time at 1100°C and employing more rapid quenching. A typical record of the X-ray analysis of steels S4 and S5 is shown in Table II.

The diffraction lines for the ferrite phase were stronger in steel S3 than in steel S4.

Table III gives the results of X-ray analysis and metallographic examination of the transformed specimens. The phases were identified by X-ray powder analysis of the steels and their extracted residues. The corresponding microhardness data are also given against each phase.

Precipitates from steels given the standard anneal at 1100°C for 30 min were extracted electrolytically and analysed by X-ray diffraction. These precipitates were found chiefly to consist

TABLE II X-ray analysis of steels annealed at 1100°C for 30 min.

Steel S4				Steel S5			
d (Å)	I/I_0	hkl	Phase	d (Å)	I/I_0	hkl	Phase
2.090	v.s.	(111)	gamma	2.095	v.s.	(111)	gamma
2.033	f	(110)	alpha	—	—	—	—
1.809	s	(200)	gamma	1.796	s	(200)	gamma
1.278	s	(220)	gamma	1.271	s	(220)	gamma
1.175	v.f.	(211)	alpha	—	—	—	—
1.089	v.s.	(311)	gamma	1.084	v.s.	(311)	gamma
1.043	s	(222)	gamma	1.039	s	(222)	gamma

v.s. = very strong line, s = strong, f = faint, and v.f. = very faint.

TABLE III Phase structure as related to time and temperature.

Temperature	Time	Steel S3		Steel S4		Steel S5	
		Phase	Microhardness (DPN)	Phase	Microhardness (DPN)	Phase	Microhardness (DPN)
1400°C	30 min	γ δ	291 349	γ δ	259 336		
1280°C	20 min	γ δ	310 335	γ δ	235 340	γ	217
1200°C	15 min	γ δ	272 310	γ δ	233 386		
1100°C	30 min	γ δ	270 400	γ (δ)	277 —		
900°C	30 min	—	—	γ (B) (α)	310 — —		
	2 h	γ (δ)	241 —	γ (B) (δ)	319 — —		
	6 h	γ (δ)	247 —	γ (B) (δ)	319 421 —	γ	228
800°C	21 h	B γ	354 241	γ B	339 443		
700°C	17 h	B (γ)	400 —	γ B	362 460		
	100 h	α with general ppt.	490	γ B	305 460	γ	245

(i) Round bracket represents minor phases; (ii) 'B' is an aggregate of (α + Cr_2N).

of Cr_2N, with small quantities of $Cr_{23}C_6$ and Fe_2N. This was confirmed by chemical analysis of the residue which showed chromium and nitrogen to be the major constituents. Table IV gives the result of X-ray analysis of the residue extracted from steel S3 after annealing at 1100°C for 30 min.

Similar results were obtained for steels S3 and S4 at different temperatures of ageing.

4. Discussion

The results obtained will be discussed, starting with the annealed steels followed by those treated at 1400°C and successively lower temperatures.

4.1. Annealed at 1100°C

The structure of steels S3 and S4 is shown in figs. 1, 2a and b. The absence of grain boundary ferrite allotriomorphs may be noticed. Both steels show an austenitic matrix with two types of ferrites:

(*a*) An acicular Widmanstätten ferrite. The length of these plates is oriented in a direction favourable to growth in the austenite grain; side thickening and branching also occur in them. The plates show a high hardness and metallographic examination shows some sort of precipitate inside the plates, the nature of which is not clear. The microhardness of this acicular ferrite is about 400 DPN.

(*b*) A plate-like ferrite marked "A" in figs. 2a and b. This consists of elongated particles of ferrite. This type of ferrite occurs in a colony, a single austenite grain normally having a single colony in which all the ferrite particles are oriented in the same direction. Usually this mode of transformation starts from a grain boundary, but sometimes also from the side of the Widmanstätten plate. This transformation is the result of ferrite nucleating at several places and the growth occurs along particular planes. The colony advances by formation of fresh nuclei of ferrite. During this process a redistribution of alloying elements occurs among the two phases. The ferrite becomes richer in Cr, whereas the

surrounding austenite in C, N and Mn. The austenite therefore becomes more stable and this may be the reason that fresh nuclei of ferrite are formed in preference to the growth of existing particles. The microhardness of these particles of ferrite is about 325 DPN.

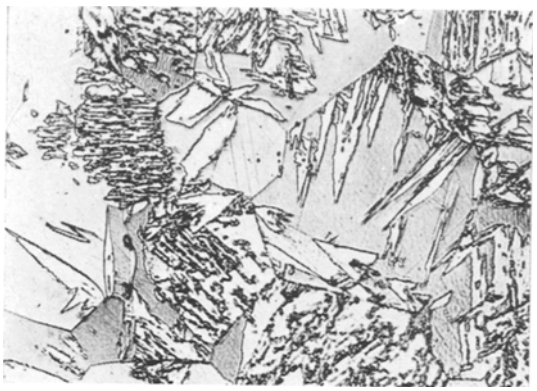

Figure 1 Steel S3, 1100°C – 30 min (× 730).

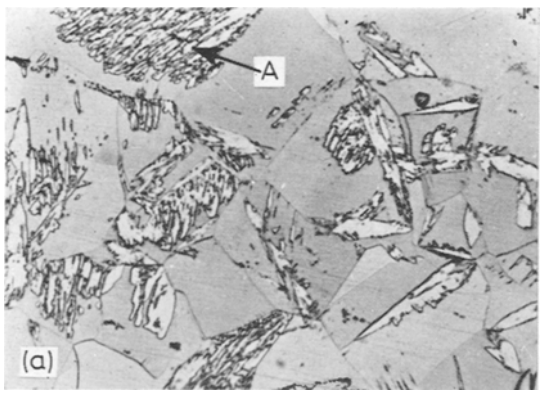

Figure 2 (a) Steel S4, 1100°C – 30 min (× 190).

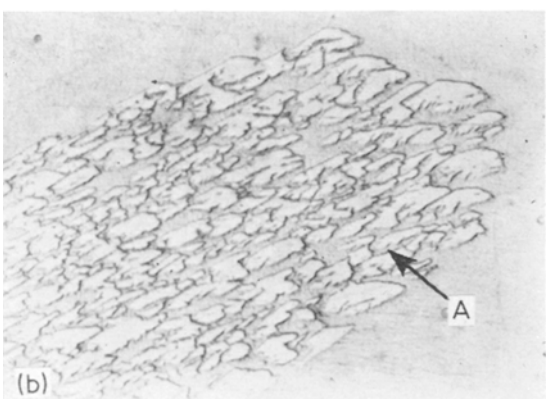

Figure 2 (b) Steel S4, 1100°C – 30 min (× 1530).

Figures 1, 2(a) and *2*(b) Acicular Widmanstätten ferrrite and plate-like ferrite (marked "A") in the matrix of austenite.

The formation of the two kinds of ferrite indicates that the starting material must have been richer in γ phase, part of which transforms to δ phase on heating to 1100°C. These steels were forged starting from 1200°C to much lower temperature of about 950°C. At these lower temperatures the steels have considerably more γ phase. This is to be expected from a steel whose composition lies in the $\alpha + \gamma$ region. This γ phase subsequently transforms to δ phase on heating to higher temperatures.

In the case of steel S4 with 8% Mn, the growth of the ferrite plates is restricted as compared to S3. In steel S5 with 10% Mn, no such reaction is observed. This shows the stabilisation effect of manganese on the austenite matrix.

4.2. At 1400°C

Both steels S3 and S4 show ferrite in a matrix of austenite (figs. 3 and 4). The absence of Widmanstätten plates will be noticed.

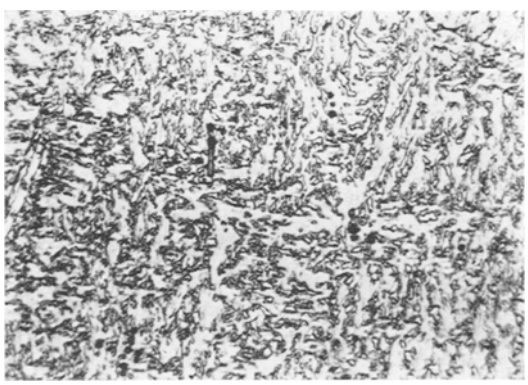

Figure 3 Steel S3, 1400°C – 30 min (× 350).

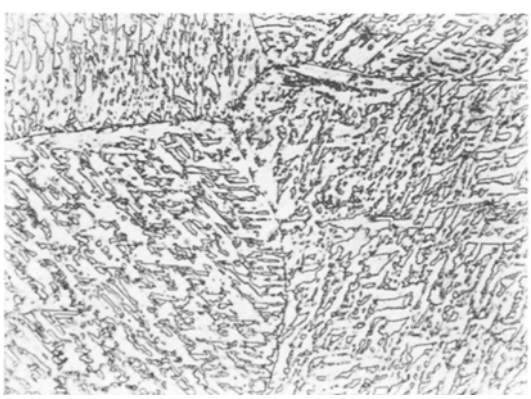

Figure 4 Steel S4, 1400°C – 30 min (× 350).

Figures 3 and *4* Ferrite in a matrix of austenite.

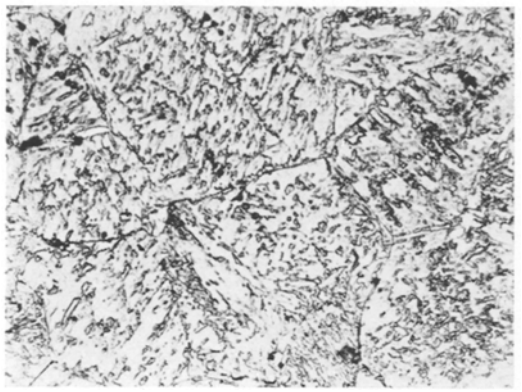

Figure 5 Steel S3, 1280°C – 20 min (× 350). δ-ferrite in the matrix of austenite.

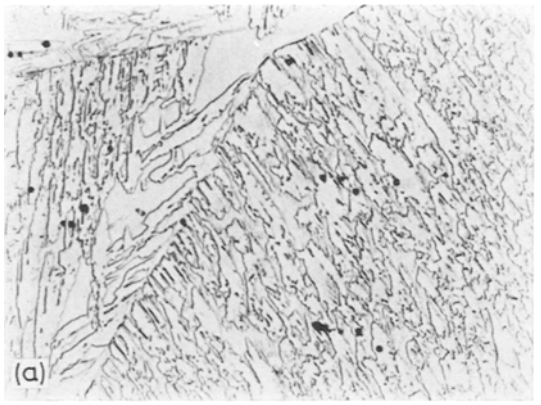

Figure 6 (a) Steel S4, 1280°C – 20 min (× 350). δ-ferrite in austenite matrix.

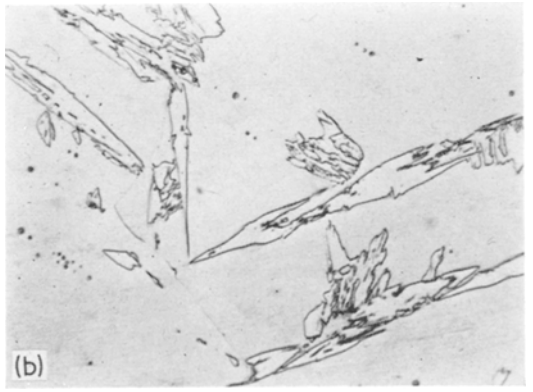

Figure 6 (b) Steel S4, 1280°C – 20 min (× 350). Widmanstätten delta ferrite.

4.3. At 1280°C

At some places allotriomorphs of delta ferrite are observed in steel S3 at the grain boundaries of the matrix austenite (fig. 5). The delta ferrite formed in this steel is stable and does not transform during quenching to the products reported in steels of 17% Cr composition without manganese and nitrogen additions [5].

The 8% Mn steel S4 (fig. 6) at 1280°C shows both types of delta ferrite. Grain coarsening can be noticed. Fig. 6a shows some Widmanstätten δ-ferrite.

4.4. At 1200°C

Both steels S3 and S4 at 1200°C (figs. 7 and 8) show the same features as at 1280°C.

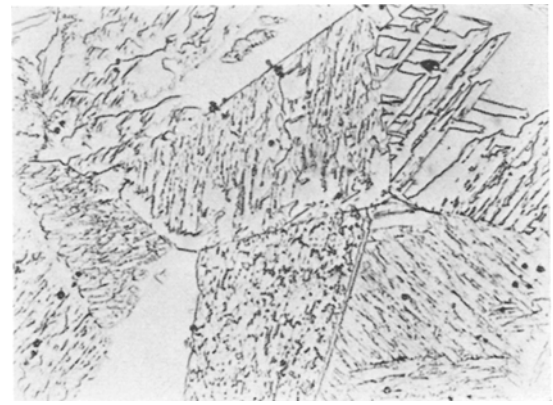

Figure 7 Steel S3, 1200°C – 15 min (× 350).

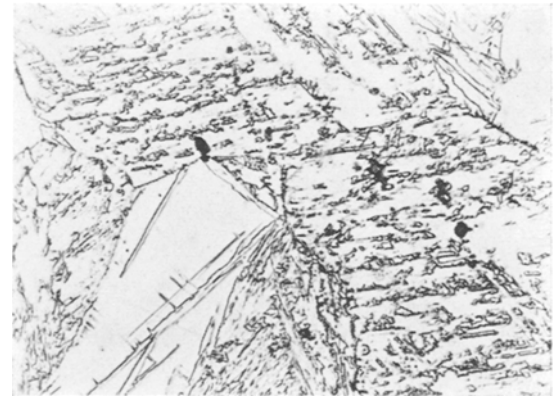

Figure 8 Steel S4, 1200°C – 15 min (× 350).

Figures 7 and *8* Same features as shown for 1230°C.

4.5. At 900°C

On isothermal holding for 2 h, steel S3 (fig. 9a) retains the same features as found in the steel treated at 1100°C for 30 min. However, on isothermal treatment for 6 h (fig. 9b), the δ-ferrite phase dissolves in the austenite matrix and a new aggregate starts forming at the grain boundaries of austenite.

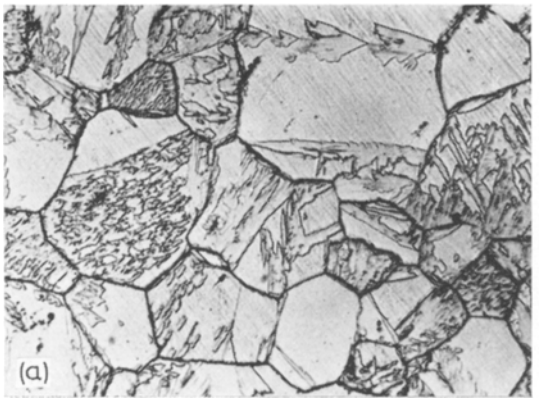

Figure 9 (a) Steel S3, 900°C – 2 h (× 190). Acicular Widmanstätten ferrite and plate-like ferrite in austenite matrix.

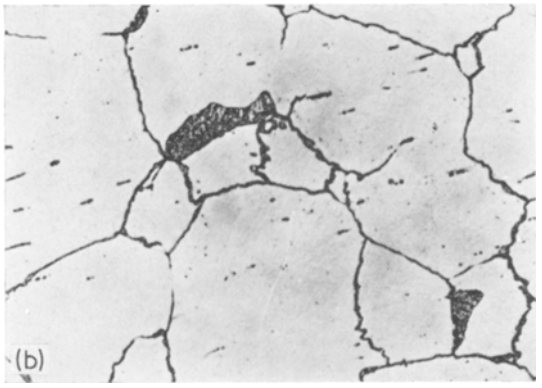

Figure 9 (b) Steel S3, 900°C – 6 h (× 190). Dissolution of δ-ferrite in the austenite matrix and formation of B-aggregate at the grain boundaries.

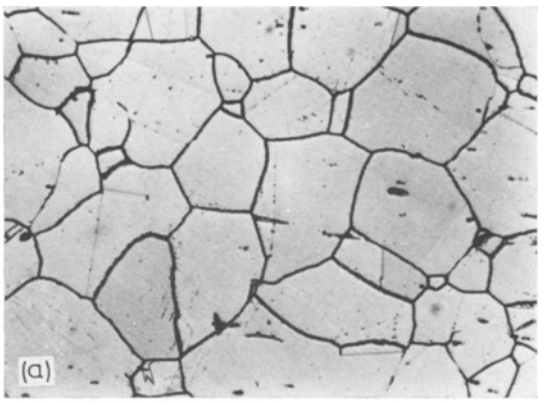

Figure 10 (a) Steel S4, 900°C – 2 h (× 190).

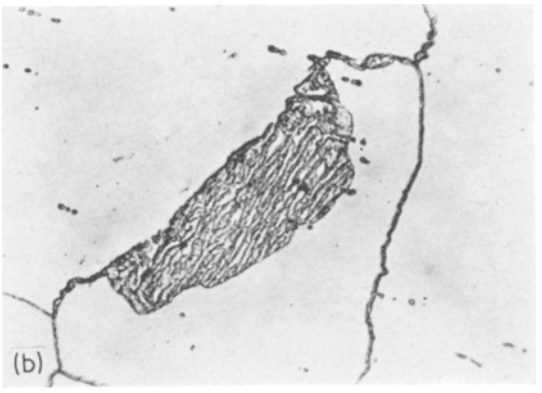

Figure 10 (b) Steel S4, 900°C – 2 h (× 980).

Figure 10 (a and b) Beginning of the formation of B-aggregate.

In steel S4, some ferrite is still seen after isothermal treatment for 30 min. On further holding for 2 h, the structure changes completely to gamma phase and a new aggregate starts forming at preferred regions of the austenite grain boundaries (figs. 10a and b). These new aggregates that form in steels S3 and S4 at this temperature are the B-aggregates (or nitrogen-pearlite) as named by Castro and Tricot [5], and consist of alternate lamellae of α ferrite and Cr_2N.

4.6. At 800°C

The nature of B-aggregate can be clearly seen in steels S3 and S4 aged at 800°C (figs. 11 and 12). In steel S3, the rate of $\gamma \rightarrow \alpha$ transformation is so fast that the structure consists of ferrite as the major phase. In steel S4 (8% Mn), the same reaction is observed, but austenite continues to be the major phase. This again shows the stabilising effect of Mn.

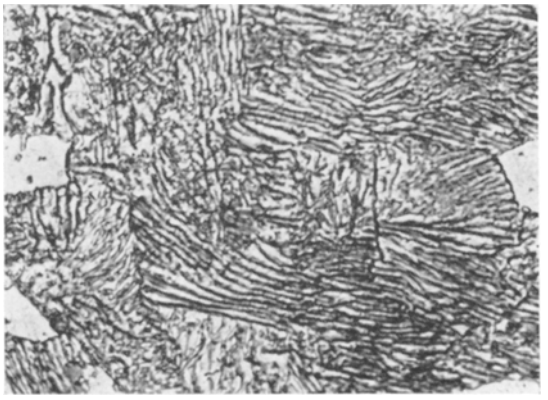

Figure 11 Steel S3, 800°C – 21 h (× 980). B-aggregate.

4.7. At 700°C

Whereas steel S3 on ageing for 100 h transforms

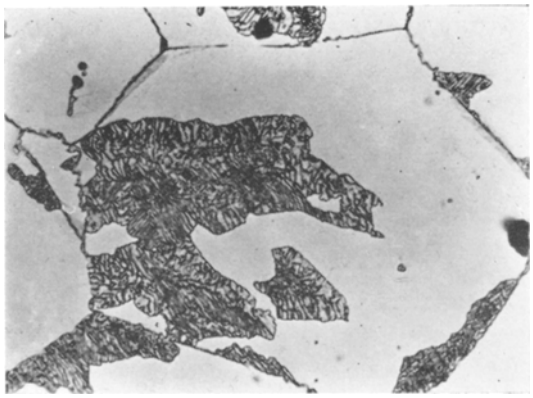

Figure 12 Steel S4, 800°C – 21 h (× 350). B-aggregate in austenite matrix.

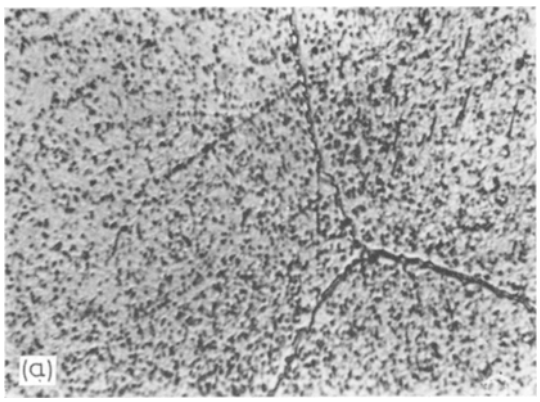

Figure 13 (a) Steel S3, 700°C – 100 h (× 980).

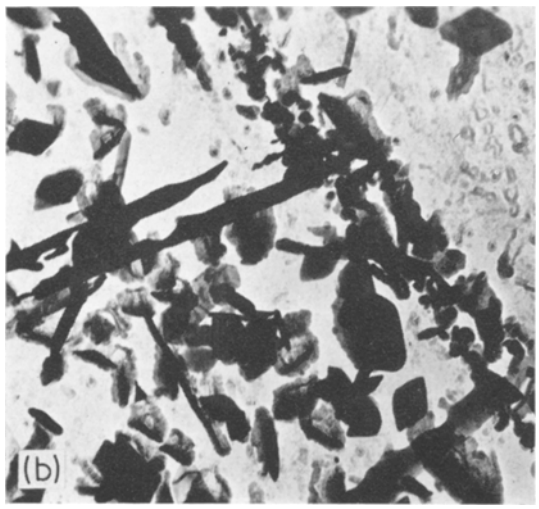

Figure 13 (b) Steel S3, 700°C – 100 h (carbon replica) (× 30000).

Figure 13 (a and b) Dispersion of Cr_2N in α-ferrite.

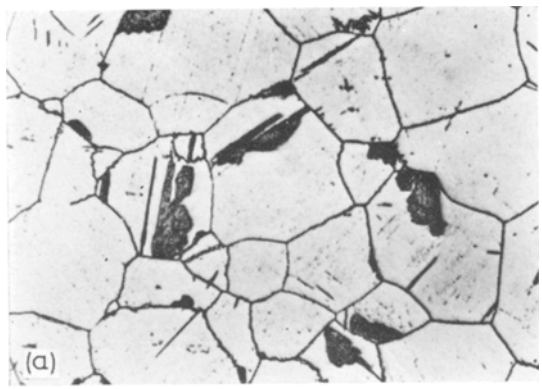

Figure 14 (a) Steel S4, 700°C – 100 h (× 350).

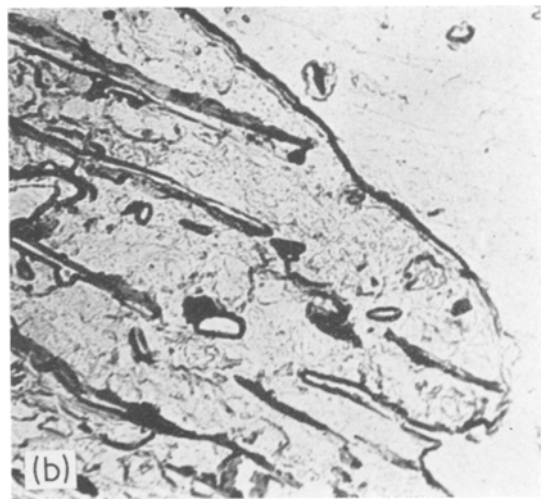

Figure 14 (b) Steel S4, 700°C – 100 h (Ni-C replica) (× 20000).

Figure 14 (a and b) B-aggregate along the grain boundaries in austenite matrix.

completely into α-ferrite with a fine dispersion of Cr_2N (figs. 13a and b), the steel S4 (figs. 14a and b) shows the same behaviour as observed in the case of 800°C treatment (fig. 12). The B-aggregate in steel S4 is formed at the grain boundaries. Steel S3 recorded a very high hardness of 500 VPN after ageing at 700°C for 100 h.

5. Mechanism of Transformation

On the basis of these experiments some inferences can be drawn on the mode of the decomposition of these steels. These can be enumerated as follows.

5.1. Austenitic Steels

Fig. 15 for a 10% Mn steel (S5) shows only a grain boundary precipitation, despite 100 h

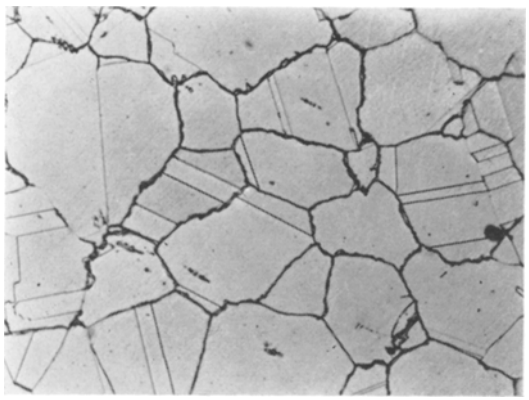

Figure 15 Steel S5, 700°C – 100 h (× 350). Completely austenitic phase with g.b. precipitation of $Cr_{23}C_6$.

TABLE IV X-ray data of electrolytically extracted precipitate.

d (Å)	I/I_0	Phase
2.422	v.f.	Cr_2N
2.238	m	Cr_2N
2.163	m	$Cr_{23}C_6$
2.125	v.s.	Cr_2N
1.640	m	Cr_2N
1.268	m	Cr_2N
1.162	f	Fe_2N
0.934	f	Fe_2N

v.s. = very strong, m = medium, f = faint, and v.f. = very faint.

treatment at 700°C. The precipitate was identified to be $Cr_{23}C_6$ by X-ray diffraction analysis. This is in agreement with the findings of Hsiao and Dulis, who also did not observe any general precipitation of the carbide phase when the carbon content of the steels was maintained below 0.15% [6]. A remarkable feature of the microstructure of 10% Mn austenitic steels investigated by us, is the absence of any discontinuous precipitation in contrast with the findings of other workers for steels which are similar but have different Cr, C and N contents [7-9].

The addition of Mn to chromium steels does not appreciably widen the gamma field at low carbon content, its effect being principally that of stabilising the austenite which is formed at high temperatures by lowering its critical cooling rate and by making it more resistant to prolonged tempering.

5.2. Steels with Unstable Austenite Structure

When the Mn content of steels is less than 10% at the same level of (C + N) of ~ 0.4%, an unstable austenite is formed.

In the case of steel S3, isothermal holding at 1280°C causes the formation of δ-ferrite from austenite. The formation of δ-ferrite leads to a redistribution of the alloying elements amongst the phase constituents [10]. One would expect Cr concentration to increase in the δ phase and C and N in the γ phase. The growth of the ferrite plate would, therefore, be opposed. At higher temperature it has been noticed that fresh nuclei of ferrite are favoured as compared to growth of the existing particles.

At holding temperatures below 900°C, the austenite phase becomes unstable and starts transforming by a discontinuous reaction into alternate lamellae of Cr_2N and α-ferrite. As the temperature is progressively lowered, the amount of the nitrogen-pearlite increases. Fig. 13 shows the microstructure of steel S3 aged at 700°C for 100 h. Austenite has completely transformed and the structure is entirely ferritic with continuous precipitation of finely divided Cr_2N. Fig. 14 (S4) aged for 100 h at 700°C shows regions of discontinuous precipitates in a matrix of untransformed austenite. The stabilising effect of Mn on austenite is apparent.

As the surface energy necessary for the formation of a nucleus is less at the grain boundary, the interfaces are suitable sites for the precipitation to occur. The formation of δ-ferrite takes place at the austenite grain boundaries between 1200 and 900°C.

6. Conclusions

A study of the structures of some 17% Cr (Mn, N) stainless steels has shown that the steels containing 10% Mn and about 0.4% N + 0.1% C are entirely austenitic. Like other austenitic stainless steels, a grain boundary precipitation of $Cr_{23}C_6$ occurs, but a remarkable feature is that no other form of precipitation, i.e. general or discontinuous precipitation (a common phenomenon in Cr-Mn-N stainless steels) is observed. This may be attributed to the optimum level of nitrogen which is retained in solution at different temperatures. This observation could be significant in the production of such steels and their behaviour in service.

Steels containing less than 10% Mn form an unstable austenite which undergoes transformation with time. The various stages observed at decreasing temperatures are

(i) Formation of δ-ferrite acicular needles and

particles in colonies at 1100°C. At higher temperatures the formation of acicular needles decreases and the formation of ferrite particles is favoured.
(ii) Transformation to γ (900°C).
(iii) Decomposition of the austenite into a lamellar aggregate of α-ferrite and Cr_2N (800°C).
(iv) Continuous precipitation of finely divided Cr_2N in the matrix of α-ferrite in 6% Mn steel at 700°C. This does not happen in 8% Mn steel.

Acknowledgement

The authors are grateful to Dr V. A. Altekar, Director, National Metallurgical Laboratory, Jamshedpur for permission to publish this paper.

References

1. S. S. BHATNAGAR, "Low-Nickel and Nickel Substantive Free Stainless Steels". Ph.D. Thesis, Banaras Hindu University (India), 1962.
2. M. HANSEN and K. ANDERKO, "Constitution of Binary Alloys" (McGraw-Hill, New York, 1958) p. 525.
3. E. J. WHITTENBERGER, E. R. ROSENOW, and D. J. CARNEY, *Trans. AIME* **209** (1957) 889.
4. K. J. IRVINE, D. T. LLEWELLYN, and F. B. PICKERING, *J. Iron & Steel Inst.* **192** (1959) 218.
5. R. CASTRO and R. TRICOT, *Metal Treatment* **31** (1964) 401. *ibid* **31** (1964) 469.
6. C. M. HSIAO and E. J. DULIS, *Trans. ASM* **50** (1958) 773.
7. G. HENRY and J. PLATEAU, *Nat. Metall. Lab.* (India), *Tech. J.* **5** (1963) 25.
8. E. J. DULIS, "Metallurgical Developments in High Alloy Steels" (ISI Special Report 86, London 1964) p. 162.
9. J. K. MUKHERJEE and B. R. NIJHAWAN, *J. Iron & Steel Inst.* **205** (1967) 62.
10. A. E. NEHRENBERG and P. LILY, *Trans. ASM* **46** (1954) 1176.

Received 3 April 1970 and accepted 11 January 1971.

Letters

Generating Electron Channelling Patterns in the JSM-II SEM

A detailed analysis has recently been carried out on the electron optical conditions for generating single crystal electron channelling patterns (ECP's) in the JSM-II scanning electron microscope [1]. Because of the large number of such SEM's currently in service and because of the rising interest in the electron channelling pattern technique, the analysis is summarised here. A general analysis was reported earlier [2] and applied specifically to the "Stereoscan"; the geometry of the JSM-II is sufficiently different to warrant a separate study. The origin and applications of ECP's have been discussed quite extensively in the literature, and the reader is referred to a recent review by Dr G. R. Booker [3]. Suffice it to say that patterns are comprised of orientation dependent lines and bands of contrast, which arise through variations in the back-scattered and secondary emitted electron intensities as the incident beam scans through the reflecting positions for various Bragg planes. ECP's are useful for determining accurately crystal orientations and for assessing crystal (near-surface) perfection.

The important requirements are small beam divergence δ and high beam current i at the specimen. For a practical guide we assume the values $\delta \leqslant 3 \times 10^{-3}$ radians and $i \gtrsim 10^{-9}$ amps. These can be satisfied in several ways depending on the type of beam required. For instance, a narrow focused beam is used to generate simultaneously channelling contrast and contrast from surface features; a wide collimated beam is used for patterns only, since it integrates out of the image contrast due to topographical and other features of repeat distance smaller than about half the beam diameter; an unfocused beam is used only if there are no surface features. The procedures follow:
(*a*) For an unfocused beam the simplest method is to turn off the lenses. The divergence in radians is then given by $\delta = (D_2/800) \times 10^{-3}$ where D_2 is the diameter in microns of the final aperture, and the beam current is given by $i = \beta D_2^2 \delta^2$ where β is the gun brightness ($\approx 2 \times 10^1$ amps/cm^2-sr. at 25 kV); the beam size 1_2 is essentially D_2. For a standard JSM-II, $D_2 \approx 200$ μm.
(*b*) For a focused beam the condenser (lens 1) is operated at long focal length by removing the pole-piece, and the objective (lens 2) is used to focus the beam to a spot onto the specimen. To prevent cut-off during scanning of the beam (now narrow in the plane of lens 2) the final aperture is enlarged, and to satisfy divergence requirements the first aperture, usually about 1 mm, is reduced. In this case $\delta = [U_2 D_1/30\ (220\text{-}U_2)] \times$